

Article

Selective Synthesis of a Gasoline Fraction from CO and H₂ on a Co-SiO₂/ZSM-5/Al₂O₃ Catalyst

Roman E. Yakovenko ^{1,*}, Grigory B. Narochnyi ¹, Ivan N. Zubkov ¹, Ekaterina A. Bozhenko ¹, Yash V. Kataria ¹, Roman D. Svetogorov ² and Alexander P. Savost'yanov ¹

¹ Research Institute "Nanotechnologies and New Materials", Platov South-Russian State Polytechnic University (NPI), Prosveshchena 132, 346428 Novocherkassk, Russia; narochgb@bk.ru (G.B.N.); 71650021.qwe@mail.ru (I.N.Z.); bogenkoekaterina@mail.ru (E.A.B.); katariaiyash1603@gmail.com (Y.V.K.); savostap@mail.ru (A.P.S.)

² National Research Center "Kurchatov Institute", 1 Akademika Kurchatova Square, 123098 Moscow, Russia; rdsvetov@gmail.com

* Correspondence: jakovenko@lenta.ru

Abstract: This article reports on a simple method for producing high-octane gasoline from CO and H₂ on a Co-Al₂O₃/SiO₂/HZSM-5/Al₂O₃ hybrid catalyst. In the selected pressure range (0.5, 1.0, and 2.0 MPa), it was found that a decrease in pressure and an increase in temperature contribute to an increase in the content of branched hydrocarbons. The optimal technological parameters of the process were determined to ensure high selectivity and productivity for C₅–C₁₀ hydrocarbons: pressure—1.0 MPa, ratio H₂/CO = 2, gas space velocity—1000 h^{−1}, temperature—250 °C. The selectivity for the gasoline fraction is 65.2%, and the ratio of branched to linear hydrocarbons (iso/n index) is 2.3. Under the specified technological conditions, an experimental batch of gasoline fraction (1000 cm³) was produced at the pilot plant during 400 h of continuous operation. The main physicochemical and operational parameters of the experimental gasoline fraction of hydrocarbons have been determined. The octane number determined by the research method according to GOST R 52947-2019 is 78.5 units.

Keywords: Fischer–Tropsch synthesis; bifunctional cobalt catalyst; HZSM-5 zeolite; synthetic gasoline fuel



Citation: Yakovenko, R.E.; Narochnyi, G.B.; Zubkov, I.N.; Bozhenko, E.A.; Kataria, Y.V.; Svetogorov, R.D.; Savost'yanov, A.P. Selective Synthesis of a Gasoline Fraction from CO and H₂ on a Co-SiO₂/ZSM-5/Al₂O₃ Catalyst. *Catalysts* **2023**, *13*, 1314. <https://doi.org/10.3390/catal13091314>

Academic Editor: Valeria Di Sarli

Received: 11 August 2023

Revised: 13 September 2023

Accepted: 14 September 2023

Published: 21 September 2023



Copyright: © 2023 by the authors. Licensee MDPI, Basel, Switzerland. This article is an open access article distributed under the terms and conditions of the Creative Commons Attribution (CC BY) license (<https://creativecommons.org/licenses/by/4.0/>).

1. Introduction

Recently, there has been a growing interest in technologies for the industrial production of liquid hydrocarbons, in particular, synthetic gasoline, from non-oil raw materials (natural gases, coal, biomass) [1–3]. The first industrial-scale production of synthetic gasoline using the Fischer–Tropsch (FT) method was mastered at Ruhrchemie in Germany during the Second World War [4]. The gasoline fraction of hydrocarbons synthesized at the plants was mainly represented by linear paraffins and olefins and had a low octane number, about 40–50 units. The technology was multi-stage and very costly and, in the future, could not compete with motor fuels produced from natural oil [5].

Currently, large-scale production of synthetic hydrocarbons based on the synthesis of FT makes it possible to obtain a low-octane gasoline fraction (naphtha), which is sent for further processing or used as a feedstock for petrochemicals, solvents, etc. It is possible to obtain high-octane gasoline from CO and H₂ using MTG technology (methanol to gasoline), involving the synthesis of methanol, on which dimethyl ether is based, followed by the conversion of the latter into hydrocarbons. MTG technology is a three–Mobil process [6], two–TIGAS process [7], or one-stage technological process [8]. The main products of this technology are hydrocarbons of the gasoline fraction, which consist mainly of aromatic, branched paraffin and cycloparaffin hydrocarbons [9,10]. The octane number of the gasoline fraction obtained by these processes can reach 90 units.

In the synthesis of hydrocarbons using the FT method on zeolite-containing catalysts, the selectivity for the gasoline fraction, depending on the synthesis conditions, varies from 60 to 90% [11–18]. At the same time, it is important that the synthesis products contain a significant proportion of iso-alkanes, which have high antiknock properties. For example, in a commercial catalyst developed by Chevron, the selectivity for the fraction C₅–C₂₀ is 71.8%, but the content of iso-alkanes in the synthesis products is not indicated [19].

Previously, we developed a bifunctional cobalt catalyst for the synthesis of FT for the direct production of liquid hydrocarbons from synthesis gas [20,21]. On this catalyst at a pressure of 1.0–2.0 MPa, light synthetic oil is obtained, consisting of gasoline and diesel fractions. The purpose of this work is to search for synthesis conditions under which the gasoline fraction obtained on this catalyst is enriched in iso-alkanes, which have high antiknock properties.

2. Results and Discussion

An XRD study of the catalyst (Figure 1) showed that the catalyst contains phases of Co₃O₄ oxides (reflexes in the range $2\theta \approx 10^\circ$ – 55°), ZSM-5 zeolite (reflexes in the range of angles $2\theta \approx 2^\circ$ – 12°), Al₂O₃ (reflexes at $2\theta \approx 20.3^\circ$, 29.5° , and 52.0°) formed during the heat treatment of boehmite, and SiO₂, which is X-ray amorphous. The particle size of Co₃O₄ was determined using the Debye–Scherrer equation, which was then used to determine the size of metallic cobalt d(Co⁰), the size of which was 8 nm.

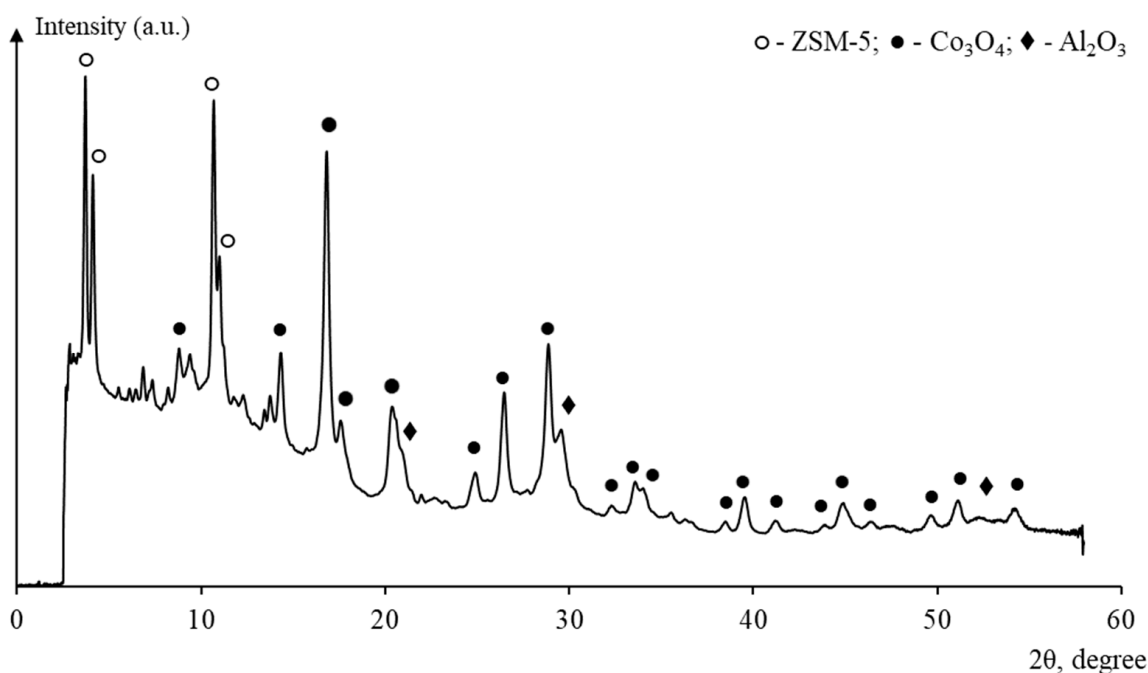


Figure 1. X-ray diffraction pattern of the catalyst in the oxide form.

It was determined using TEM that cobalt particles 3–13 nm in size were present on the catalyst surface (Figure 2); the average size was 8 ± 2 nm (Table 1).

The study of morphology using SEM (Figure 3) confirmed the heterogeneity of the state of the catalyst surface. It was found that silicon, aluminum, and oxygen atoms were more uniformly distributed over the catalyst surface, while cobalt atoms were localized fragmentarily.

According to the BJH data (Figure 4), the maximum pore-size distribution in the region of 1.5–2.5 nm corresponds to the H-ZSM-5 zeolite, and the maximum at 5 nm corresponds to the Co–Al₂O₃/SiO₂ catalyst. In the region of 6–15 nm, the catalyst has a maximum because of the presence of a binder in its composition.

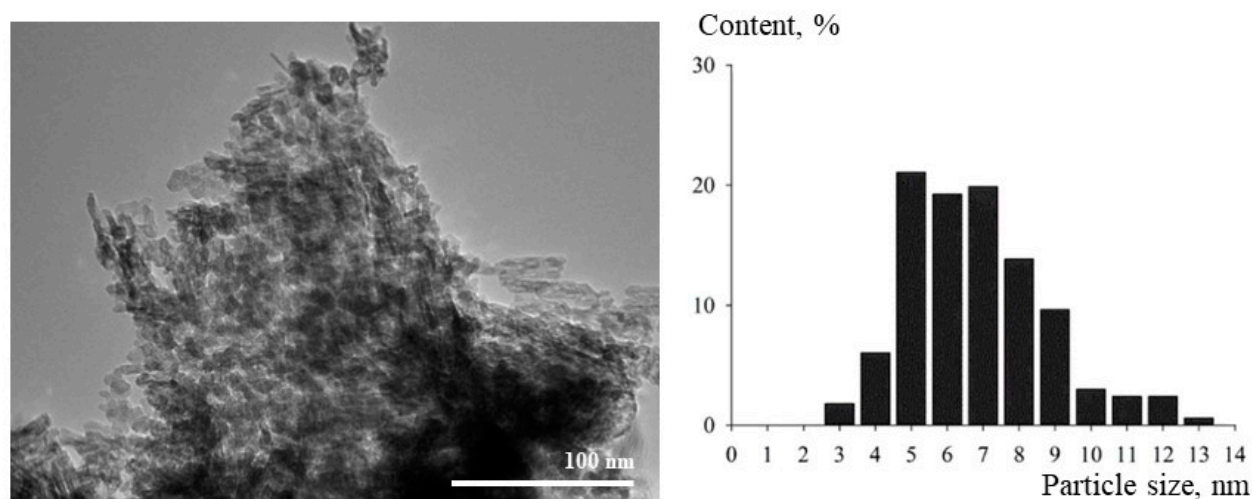


Figure 2. TEM micrograph of the reduced catalyst and histogram of cobalt particle size distribution.

Table 1. Physicochemical properties of the catalyst.

Characteristics of the Porous Structure				Co ⁰ Particle Size, nm	
S _{BET} , m ² /g	S _{EXT} , m ² /g	V _{micro} , cm ³ /g	V _Σ , cm ³ /g	XRD	TEM
245	187	0.03	0.59	8.0	8 ± 2

Note: S_{BET}—BET specific surface area; S_{EXT}—external specific surface; V_{micro}—specific volume of micropores; V_Σ—total pore volume.

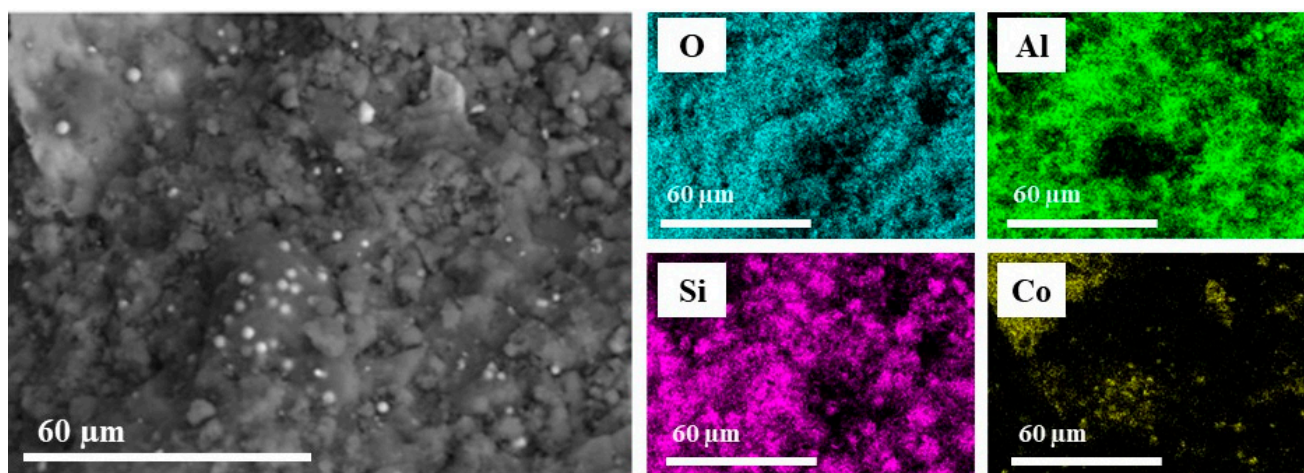


Figure 3. SEM micrographs of the catalyst in the oxide form.

The specific surface area of the catalyst according to BET was 245 m²/g and was mainly determined by the presence of a zeolite and a cobalt-containing component (Co-Al₂O₃/SiO₂) in the catalyst. The share of micropores was 5% of the total pore volume.

According to the results of the TPR H₂ (Figure 5), the reduction of the cobalt-containing component of the bifunctional catalyst proceeds sequentially according to the schemes Co₃O₄ → CoO and CoO → Co⁰, which confirms the presence of two stages of reduction [22]. The ratio of peak areas of hydrogen absorption required for the reduction of Co³⁺ oxides to Co⁰ differs from the theoretically expected calculated value and is 2.70. The absence of a large H₂ absorption peak in the high-temperature region indicates that cobalt does not form difficult-to-reduce compounds with zeolite or boehmite.

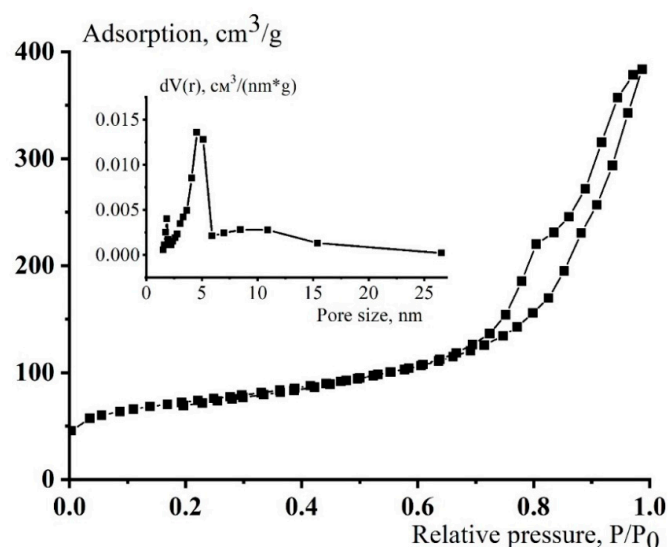


Figure 4. Nitrogen adsorption–desorption isotherms and pore-size distribution.

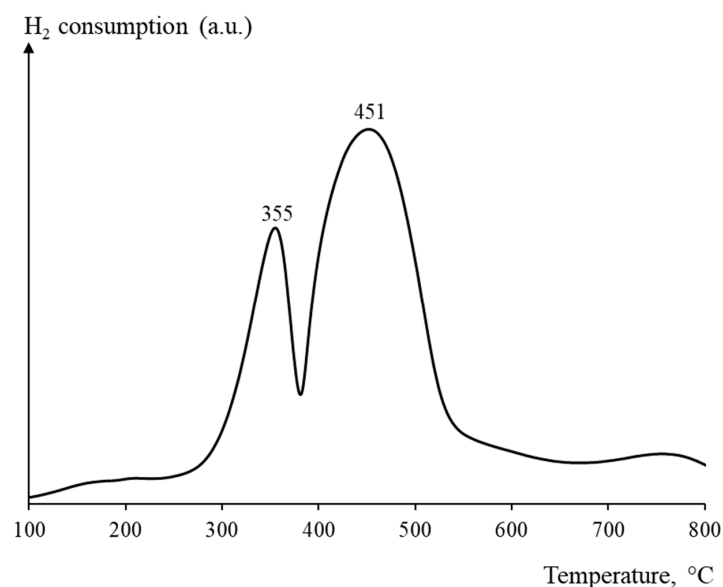


Figure 5. Curve of temperature-programmed hydrogen reduction (TPR H_2) of the catalyst.

When studying the acidity of the catalyst according to the NH_3 TPD data, it was found that the amount of ammonia desorbed in the temperature range of 100–250 °C (“weak” centers), 250–400 °C (“medium” centers), and 400–550 °C (“strong” centers) is 70 $\mu\text{mol } NH_3/\text{g}$, 31 $\mu\text{mol } NH_3/\text{g}$, and 5 $\mu\text{mol } NH_3/\text{g}$, respectively. Like the HZSM-5 zeolite, the catalyst based on it has a relatively high Bronsted acidity.

In order to select the optimal process mode and optimize the consumption coefficients of reagents for the pilot plant, the process conditions (temperature, pressure) were previously determined at the laboratory plant, under which the performance of the bifunctional cobalt FT synthesis catalyst and the selectivity for the gasoline fraction would be maximum. The criterion for the search for optimal process conditions was the presence in the synthesis products of a large number of isomeric hydrocarbon structures (high iso/n) in the synthesis products, which provide high antiknock characteristics of the gasoline fraction.

Zeolite-containing FT synthesis catalysts mainly operate in the temperature range of 230–250 °C [23–26] since, under these conditions, secondary processes of transformations of synthesized hydrocarbons on the zeolite-containing component begin to actively proceed [27]. In this study, we varied the temperature in the range of 240–250 °C. The effect

of pressure was studied in the range of 0.5–2.0 MPa under the conditions: GHSV = 1000 h⁻¹, H₂/CO ratio = 2, temperatures of 240 °C and 250 °C, and the volume of catalyst loading into the reactor of 10 cm³. The results of these studies are given in Table 2.

Table 2. Dependence of the activity and selectivity of the bifunctional cobalt catalyst for FT synthesis on pressure and temperature (GHSV = 1000 h⁻¹, H₂/CO ratio = 2).

Pressure, MPa	CO Conversion, %	Selectivity for Hydrocarbons, %		iso/n Ratio		The Ratio of o/p in the Fraction C ₅ –C ₁₀	Productivity for Hydrocarbons, kg/(m ³ _{cat} h)	
		C ₅₊	C ₅ –C ₁₀	C ₅₊	C ₅ –C ₁₀		C ₅₊	C ₅ –C ₁₀
Temperature 240 °C								
0.5	55.1	63.7	69.6	4.35	4.75	3.19	80.7	56.2
1.0	62.7	70.8	67.0	2.08	3.19	2.72	97.0	65.0
2.0	75.6	67.1	54.3	0.76	0.76	1.46	106.0	57.5
Temperature 250 °C								
1.0	74.1	70.1	73.3	2.70	3.64	2.15	113.5	83.2
2.0	85.9	72.8	62.2	1.06	1.09	1.98	130.3	81.0

Note: iso/n is the ratio of hydrocarbons of isostructure to hydrocarbons of normal structure; o/p is the ratio of alkenes to alkanes (olefins to paraffins).

A comparative analysis of the catalytic characteristics showed that with decreasing pressure, the selectivity of the catalyst for hydrocarbons in the gasoline fraction, as well as the iso/n and o/n indicators, increases. It has been established that with the technological parameters of synthesis P = 1.0 MPa, T = 250 °C, GHSV = 1000 h⁻¹, and the ratio H₂/CO = 2, selectivity and productivity for C₅–C₁₀ are 73.3% and 83.2 kg/(m³_{cat} h), respectively. Under these conditions, a significant proportion (iso/n = 3.64) of isomeric hydrocarbon structures is formed (see Table 2), which helps increase the octane number of gasoline and improve its quality characteristics. Therefore, it is advisable to produce synthetic gasoline at a pilot plant with the specified technological parameters.

Table 3 presents the average results of the hydrocarbon synthesis process at the pilot plant, obtained over 400 h of operation. During this time period, five samples of hydrocarbons were taken, which, upon completion of the synthesis, were combined into one and used to determine the average characteristics of the fuel.

Table 3. Averaged catalytic characteristics of a bifunctional cobalt catalyst for FT synthesis in a pilot plant at GHSV = 1000 h⁻¹, P = 1.0 MPa, T = 247–250 °C, H₂/CO ratio = 2.

Sample No.	Working Time, h	Average CO Conversion, % During Operation	Selectivity, %				Average Productivity According to C ₅₊ , kg/(m ³ _{cat} h)
			CH ₄	C ₂ –C ₄	C ₅₊	CO ₂	
1	0–95	78.3	19.9	12.9	65.6	1.6	113.8
2	96–161	71.2	28.9	16.3	52.7	2.1	76.9
3	162–241	76.1	27.1	15.5	55.3	2.1	87.5
4	242–340	73.6	27.8	17.1	53.1	2.0	81.2
5	341–396	71.6	33.1	16.1	46.4	4.4	69.6
1–5	0–396	75.2	26.7	15.6	55.5	2.2	86.0

With an increase in the time interval of catalyst operation, the degree of CO conversion decreased, and by the end of the experiment, it decreased by ~12% from the initial values (78.3%). The dynamics of changes in CO conversion over a time interval of 400 h is clearly shown in Figure 6.

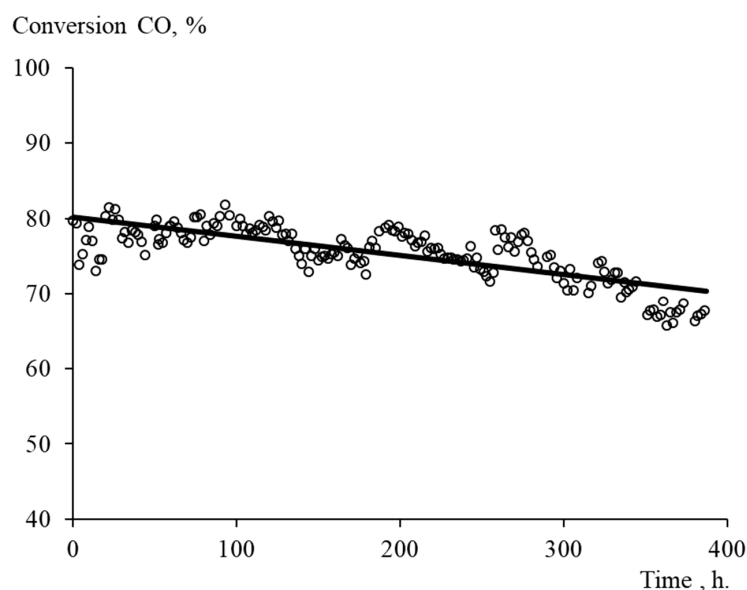


Figure 6. Dependence of CO conversion on the operating time of a bifunctional cobalt catalyst for the FT synthesis (GHSV = 1000 h⁻¹, P = 1.0 MPa, T = 245–250 °C, ratio H₂/CO = 2).

The productivity of the process over the entire period of catalyst operation decreased from 113.8 to 69.6 kg/(m³_{cat} h), and, as a result, the production of gaseous products (CH₄, C₂–C₄, CO₂) increased. The calculated average productivity of the process for the combined sample of hydrocarbons was 86.0 kg/(m³_{cat} h); that is, it decreased by 24% from the initial value. The largest decrease in productivity (by 32%) was recorded in the initial period (~100 h) of catalyst operation.

One of the factors reducing the activity can be local temperature overheating in the catalytic layer. However, temperature measurements along the height of the catalytic layer (see Figure 7) for the entire period of operation of the bifunctional cobalt catalyst for FT synthesis showed that the largest temperature gradient of 3–4 °C was observed in the initial 10 h of catalyst operation. Subsequently, it stabilized and did not exceed 2–3 °C, which indicates a sufficiently high stability of the catalyst. The main reasons for catalyst deactivation can be the agglomeration of active metal nanoparticles, as well as carburization (hydrocarbons, amorphous, and graphitized carbon) of the active catalyst surface during operation [20].

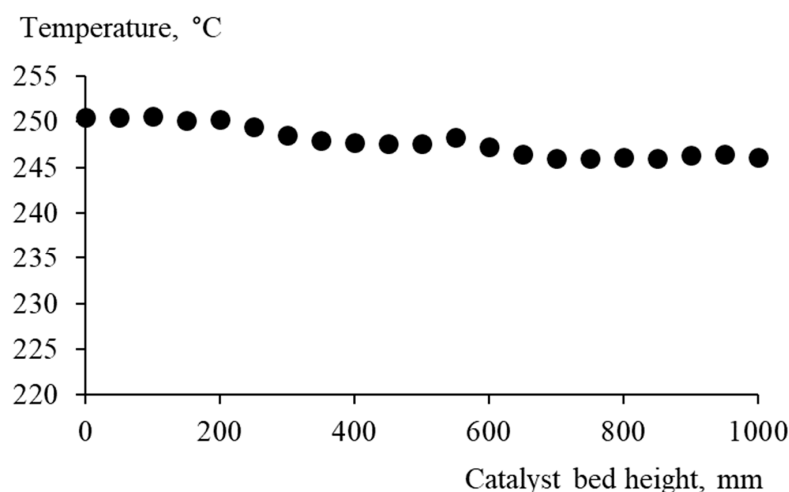


Figure 7. Temperature distribution along the height of the layer of a bifunctional cobalt catalyst for the synthesis of an FT catalyst for 400 h of operation.

Group analysis of C_{5+} products synthesized on a pilot catalytic plant showed that the average sample of hydrocarbons contains a high number of isomeric compounds; the iso/n index corresponds to a value of 2.3. The o/p index indicating the presence of unsaturated hydrocarbons in the fuel composition was 1.14 (Table 4). The molecular weight distribution diagram shows that these are predominantly branched alkenes contained in the C_5 – C_{10} gasoline fraction (Figure 8). Fuel characteristics can be significantly improved, in particular, to increase the octane properties of the fuel and reduce the content of alkenes. One of the ways to improve the performance of motor fuel is its hydro-treatment. This can be achieved by introducing promoters—hydrogenating components—into the composition of a polyfunctional catalyst [28].

Table 4. Group composition of the synthesis products of the average sample of C_{5+} hydrocarbons synthesized at the pilot plant.

Products	Group Composition of Hydrocarbons, % wt.			iso/n	o/p
	C_5 – C_{10}	C_{11} – C_{18}	C_{19+}		
<i>n</i> -alkanes	12.3	7.2	1.1	2.3	1.14
<i>Iso</i> -alkanes	14.2	10.6	1.3		
Alkenes	9.0	0.5	0.1		
<i>Branched</i> alkenes	29.7	13.7	0.3		
<i>Total</i>	65.2	32.0	2.8		

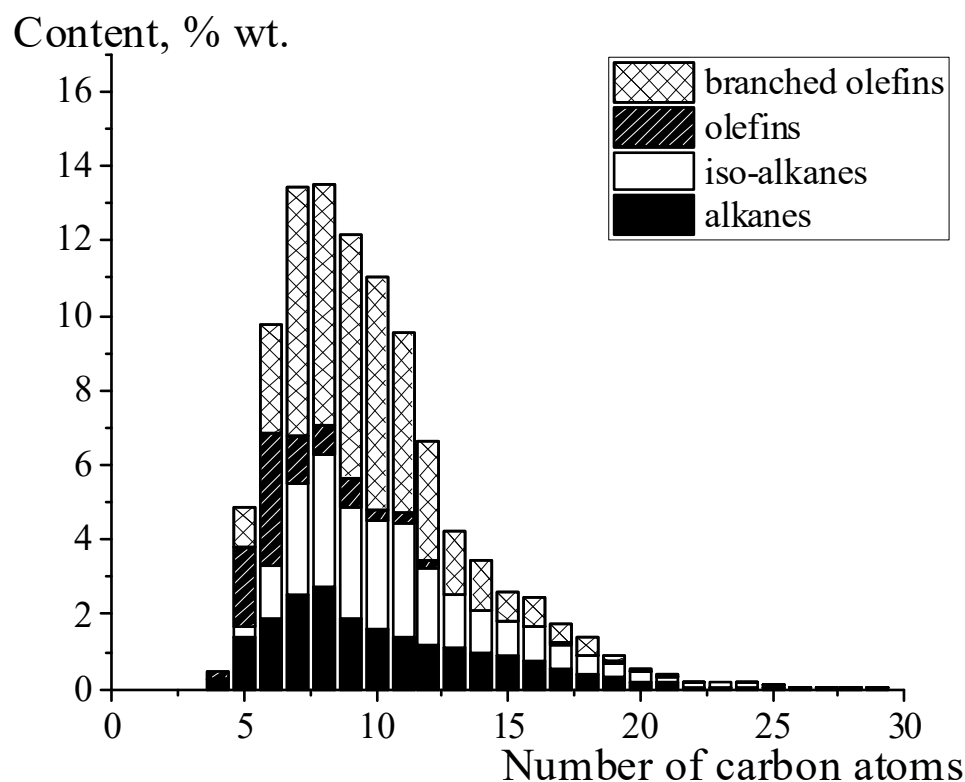


Figure 8. Molecular weight distribution of hydrocarbons in the average sample of C_{5+} hydrocarbons.

The results of a study of a number of basic physicochemical and operational indicators of a synthesized experimental batch of gasoline fraction of hydrocarbons are presented in Table 5.

Table 5. Physicochemical and operational parameters of the experimental gasoline fraction of hydrocarbons.

Indicator	Actual Value	Requirement GOST P 51105-2020	Method of Determination
Octane number (research method) not less than	78.5	92	GOST P 52947-2019
Volume fraction of benzene, %, max	absent	5.0 (1.0)	Chromatographically
Volume fraction of aromatic hydrocarbons, %, not more than	absent	42.0 (35.0)	Chromatographically
Density at 15 °C, kg/m ³	710.2	725–780	GOST P 51069-97
Net calorific value, kJ/kg	43,780	-	GOST 21261-2021
Iodine number, g of iodine per 100 g of fuel	11.8	-	GOST 2070-82
Volume fraction of hydrocarbon olefins, %, not more than	53	18	Chromatographically
Saturated vapor pressure, kPa	41.2	min. 45.0	GOST 33157-2014
Fractional composition, % vol. at temperature			
70 °C	10.2	15–50 (48)	
100 °C	39.4	40–70	GOST 2177-99
150 °C	84.7	not less than 75	
End of boiling, °C.	185.5	not higher than 215	
Volume fraction of the residue in the flask, % vol.	1.0	not more than 2.0	

Note: “-” means that the corresponding parameters are not regulated.

The octane number of the experimental gasoline fraction of hydrocarbons, determined by the research method (GOST P 52947-2019), is 78.5, which is 13.5 units lower than the minimum requirement in force by GOST. However, the obtained synthetic gasoline fraction has an octane number higher compared to the octane number of straight-run gasoline (59), hydrocracked gasoline (68), and coking gasoline (63) [29].

The density of the experimental gasoline fraction of hydrocarbons is also somewhat lower. However, the lower density of synthetic fuel, in comparison with gasoline obtained from petroleum feedstock, is due to the complete absence of aromatic hydrocarbons, which significantly improves its environmental performance.

As a rule, the calorific value of commercial gasoline is almost the same for different grades and varies within 43–44 MJ/kg [30]. The net calorific value of the obtained synthetic gasoline fuel is 43.78 MJ/kg, which is not inferior in terms of the calorific value of commercial petroleum gasoline.

An important indicator characterizing its chemical stability is the iodine number, which is determined based on the content of unsaturated compounds. The iodine number of gasoline fuel is 11.8, which corresponds to the calculated mass fraction of unsaturated hydrocarbons of 53.03 wt.%. Note that a certain proportion of unsaturated hydrocarbons, based on capillary gas–liquid chromato-mass spectrometry in the gasoline fraction of hydrocarbons, is 53.3 wt.%. However, the content of olefins significantly exceeds the requirements of the regulation. It is possible to reduce the number of olefins via light hydrogenation or, for example, the process of methoxylation to obtain esters with high antiknock resistance [31].

Fischer–Tropsch synthesis over a commercial zeolite-containing catalyst from Chevron was reported by C. Kibby et al. [19]. The developed catalyst produced C₅–C₂₀ hydrocarbons with a selectivity of 75.6%. Chuang Xing et al. [11] reported on the synthesis of zeolite-containing catalysts based on Co/SiO₂ + ZSM-5; the content of the gasoline fraction was 41.5%. In our catalyst, which was tested in a pilot reactor for almost 400 h, a larger gasoline fraction of 63.5% formed. The octane number was determined as 87 units in [11]; in our work, the octane number was determined on a single-piston unit and was 78.5 (Table 6).

Table 6. Comparison of commercial vs. synthesized catalysts.

Catalyst	P, MPa	τ , h	t , °C	X_{CO} , %	Selectivity, %								Octane Number
					CO ₂	CH ₄	C ₂ –C ₄	C ₅ –C ₁₁	C ₁₂₊	C _n	C _o	C _{iso}	
Co–Al ₂ O ₃ /SiO ₂ /HZSM-5/Al ₂ O ₃	1.0	396	250	75.2	2.2	26.7	15.6	41.5	14.0	20.5	9.5	69.9	78.5
Co/SiO ₂ + ZSM-5 [1]	1.0	6	260	67.9	2.3	13.5	20.5	63.5	2.5	43.4	19.5	37.1	87
Chevron [2]	2.0	n.d.	220	50	0.9	12.2	11.	75.6		n.d.	n.d.	n.d.	n.d.

C_n—normal paraffins; C_o—olefins (linear); C_{iso}—iso-paraffins and branched olefins.

Deactivation during the Fischer–Tropsch synthesis can be due to the phenomena of active site poisoning, formation of surface carbon and carbidization, formation of mixed compounds and re-oxidation of the metal, sintering of particles, etc.

To understand the causes of deactivation, after the reaction, we took samples of the catalyst at different heights: the top, middle, and bottom of the reactor. The selected samples were characterized with XRD using synchrotron radiation. The XRD results are shown in Figure 9.

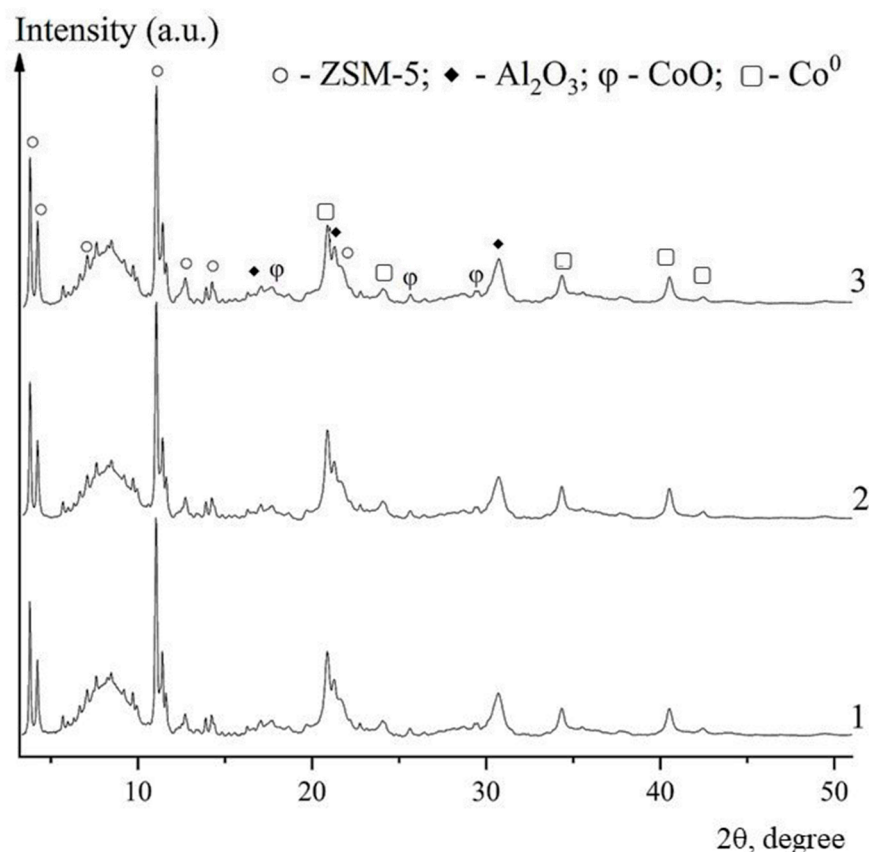


Figure 9. X-ray diffraction patterns of the catalyst after synthesis. 1—bottom layer; 2—middle layer; 3—top layer.

The diffraction pattern for all samples, regardless of the height of the catalyst layer, is of the same type: there are diffraction reflections of metallic cobalt and its oxide, aluminum oxide, and ZSM-5 zeolite. Based on XRD data, it was established that in the course of synthesis, there is no formation of hard-to-recover metal-carrier compounds and no significant oxidation of metallic cobalt. In turn, the estimated average size of crystallites of metallic cobalt is 12 nm, while the particle size of the catalyst before synthesis is 8 nm. Thus, one of the reasons for reducing the activity of the catalyst is the coarsening of particles of metallic cobalt (sintering).

3. Materials and Methods

3.1. Catalyst Preparation

A bifunctional cobalt catalyst for the synthesis of FT was obtained by mixing and molding powders of a cobalt-containing component, ZSM-5 zeolite in the H-form, and a binder, boehmite. The cobalt catalyst Co-Al₂O₃/SiO₂ was used for the selective synthesis of long-chain hydrocarbons (20.0 Co and 1.0 Al₂O₃ wt.%) with a silica gel carrier KSKG (OOO Salavat Catalyst Plant, Salavat, Russia) [22], and zeolite HZSM-5 was used as the acid component. with a SiO₂/Al₂O₃ molar ratio of 40.5 (OOO Ishimbay Specialized Chemical Plant of Catalysts, Ishimbay, Russia) [21,32] and binder boehmite Al(OH)O (Sasol, TH 80).

The catalyst was prepared by mixing the following powders (fraction <0.1 mm) in wt.%: catalyst Co-Al₂O₃/SiO₂—35, HZSM-5—30, boehmite—35 [20,21,23,32]. To plasticize the boehmite binder, an aqueous-alcoholic solution of triethylene glycol and nitric acid was used (the nitric acid solution was prepared by adding 1–2 mL of nitric acid with a concentration of 65 wt.% in 90–100 mL of distilled water per 100 g of a mixture of powders; triethylene glycol was introduced based on the volume ratio nitric acid:triethylene glycol in a mixture of 1:3). The catalyst granules were molded by extrusion. The mold was dried for 24 h at room temperature, 4–6 h at 80–100 °C, and 2–4 h at 100–150 °C and calcined for 5 h at 500 °C. To obtain an experimental batch of synthetic gasoline in a pilot plant, an enlarged laboratory batch of a bifunctional cobalt catalyst for the synthesis of FT with a volume of 500 cm³ was produced.

3.2. Catalyst Characterization

The phase composition of the reduced catalyst was determined with X-ray diffraction using the equipment of the European Synchrotron Radiation Center (ESRF, Grenoble, France) in the 2θ angle range from 5° to 55° with a radiation wavelength λ = 0.7121 Å. The determination of the qualitative phase composition was performed using PDF-2 [33] in the Crystallographica software package (Version 3,1,0,2 with RDB support). The diffraction patterns of the catalysts were processed using the FullProf program.

XRD was performed with precision X-ray diffraction using synchrotron radiation at the X-ray diffraction analysis station of the Kurchatov Research Center. The diffraction pattern was taken at a radiation wavelength of 0.074 nm using the “transmission” geometry and registration of scattered radiation with a Rayonix SX165 two-coordinate detector, LaB6 standard (NIST SRM 660a) [20]. The beam size on the sample was 400 μm. The catalyst sample was placed in a 300 μm cryostat and rotated around a horizontal axis during the measurement, which allowed the diffraction patterns to be averaged according to sample orientations.

Based on the XRD data of the catalyst in the oxide form, the average particle size of Co₃O₄ (d(Co₃O₄), nm) was determined using the Debye–Scherrer equation [34]:

$$d(\text{Co}_3\text{O}_4) = \frac{K \cdot \lambda}{\beta \cdot \cos \theta} \quad (1)$$

where d(Co₃O₄) is the average particle size (nm); K is the dimensionless particle shape factor (K = 0.89); λ is the wavelength of X-ray radiation (nm); θ is the Bragg angle (rad); β is the reflection width at half height (rad).

There is a formula that calculates, based on the average particle size of Co₃O₄ (d(Co₃O₄), nm), using the Debye–Scherrer equation to determine the size of Co⁰ particles [35]:

$$d(\text{Co}^0) = d(\text{Co}_3\text{O}_4) \times 0.75 \quad (2)$$

where d(Co₃O₄) is the average particle size of Co₃O₄ calculated using the Debye–Scherrer equation.

The particle size of the cobalt catalysts was determined through transmission electron microscopy (TEM) using a Tecnai G2 Spirit BioTWIN (FEI, Boston, MA, USA) with an accelerating voltage of 120 kV. The catalyst sample was preliminarily reduced with a

nitrogen–hydrogen mixture (5% H₂ + 95% N₂) during linear heating from room temperature to 500 °C for 1 h.

The average size of cobalt crystallites ($d_{av}(\text{Co}^0)$, nm) was calculated using the following formula [36]:

$$d_{cp}(\text{Co}^0) = \frac{\sum n_i \cdot d_i^3}{\sum n_i \cdot d_i^2} \quad (3)$$

where n_i is the number of particles with diameter d_i .

The standard deviation was determined by the following formula [36]:

$$\sigma = \sqrt{\frac{\sum_i n_i \times (d_i - d(\text{Co}^0))^2}{\sum n_i}} \quad (4)$$

The size distribution of metal particles was obtained from measurements of ~200 particles from several micrographs taken at different locations on the grid.

The microstructure of the catalyst surface was studied through scanning electron microscopy (SEM) on a JSM-6490LV microscope (JEOL, Osaka, Japan) at an accelerating voltage of 30 kV, which was equipped with an INCA Penta FET 3 energy dispersive detector (Oxford Instruments, Wycombe, UK).

The study of the parameters of the porous structure of zeolite samples was carried out via nitrogen adsorption–desorption using a Nova 1200e instrument (Quantachrome, Boynton Beach, FL, USA). The value of the specific surface obtained with the BET method (Brunauer–Emmett–Teller) was calculated at a relative partial gas pressure $P/P_0 = 0.20$. The pore volume was determined using the BJH method at a relative partial pressure $P/P_0 = 0.95$; the pore-size distribution was calculated from the BJH desorption curve (Barrett–Joyner–Halenda) the volume of micropores in the presence of mesopores was measured using the t-method (de Boer and Lippens). The samples were preliminarily subjected to vacuum treatment for 5 h at a temperature of 350 °C.

The process of reduction of surface phases and structures on the catalyst surface was studied via temperature-programmed reduction with hydrogen (TPR H₂) using a Micromeritics ChemiSorb 2750 analyzer (Micromeritics, Norcross, GA, USA) equipped with a thermal conductivity detector. TPR H₂ was carried out under the following conditions: catalyst weighed 0.10 g; gas mixture containing 10% hydrogen and 90% nitrogen; flow rate of 20 mL/min; temperature range of 20–800 °C; and heating rate of 20 °C/min. Before TPR H₂, the catalyst was kept in a helium flow (20 mL/min) for 1 h at a temperature of 200 °C to remove moisture and adsorbed gases.

The catalysts were studied via temperature-programmed ammonia desorption (NH₃ TPD) on a Quantachrome Autosorb analyzer (Quantachrome, USA). Before adsorption, the samples were degassed in a helium flow at 600 °C for 5 h and purged to remove physically adsorbed ammonia. Ammonia was adsorbed at a temperature of 100 °C in a stream of an ammonia-helium mixture (10% NH₃ by volume) for 2 h. Desorption was carried out in the temperature range of 100–600 °C with linear heating at a rate of 10 °C/min; the carrier gas was helium.

Ex situ magnetic measurements of samples were carried out on a LakeShore VSM 7404 (LakeShore Cryotronics, Westerville, OH, USA) magnetometer. Metallic cobalt is ferromagnetic at room temperature, whereas CoO is paramagnetic, so its magnetic moment can be neglected compared to the magnetic moment of the metal. Cobalt carbide is also ferromagnetic, but its magnetic susceptibility [37] is an order of magnitude lower compared to metallic cobalt [38], so it could be neglected as well. Thus, neglecting the magnetization of non-metallic cobalt phases, the fraction of metallic cobalt in total loaded cobalt in the sample $\text{Co}^0/\text{Co}^{\text{tot}}$, i.e., the cobalt extent of reduction (EOR), can be estimated from the following relation:

$$\text{EOR} = \text{Co}^0/\text{Co}^{\text{tot}} = M_s/\sigma \cdot m \quad (5)$$

where M_s is the measured saturation magnetization of a catalyst sample (emu), σ is the specific magnetic susceptibility for bulk cobalt (164 emu/g^2), and m is the cobalt mass contained in the sample (g).

3.3. Catalyst Characterization

The study of the influence of technological parameters in order to select the optimal technological mode for determining the maximum selectivity and productivity for the gasoline fraction was carried out on a laboratory installation in a flow mode in a tubular reactor (inner diameter 16 mm) with a stationary bed of a pre-reduced catalyst using synthesis gas with a ratio of $\text{H}_2/\text{CO} = 2$ at pressures of 0.5, 1.0, and 2.0 MPa, gas hourly space velocity (GHSV) = 1000 h^{-1} , and temperature of $240\text{--}250 \text{ }^\circ\text{C}$ in a continuous mode for 50–100 h. The catalyst was preliminarily reduced with hydrogen for 3 h at $400 \text{ }^\circ\text{C}$ and GHSV 3000 h^{-1} ; the degree of reduction of cobalt was 60%.

The production of a batch of gasoline fraction in a volume of at least 1 L was carried out on a pilot plant with a tubular reactor 1500 mm high. The pilot plant and its technological scheme are shown in Figure 10.

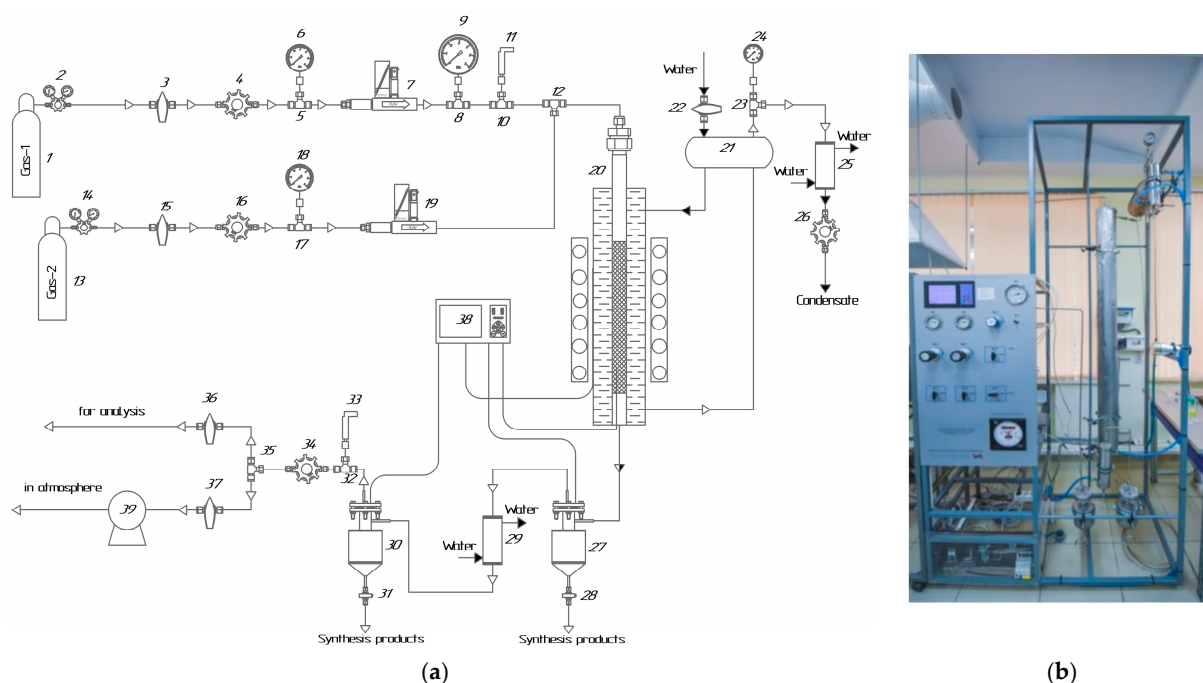


Figure 10. Technological scheme (a) and pilot plant (b): (a) 1, 13—gas cylinders; 2, 14—gas reducers; 3, 15, 22, 36, 37—shut-off valves; 4, 16, 26, 34—pressure regulators; 5, 8, 10, 12, 17, 23, 32, 35—straight tees; 6, 9, 18, 24—manometers; 7, 19—component flow regulators; 11, 33—pressure sensors; 20—synthesis reactor; 21—steam collector; 27, 30—separators; 25, 29—cooler; 28, 31—valves; 38—temperature controller “Termodat”; 39—gas meter; (b) photo of the pilot plant.

The unit consists of a reagent preparation unit, a hydrocarbon synthesis reactor unit, and a reaction product cooling unit. H_2 and CO gases are supplied from cylinders 1 and 13 installed outdoors. Control over the level of gas consumption is carried out using the Bronkhorst gas flow regulators of the EL-FLOW series in automatic mode. The reactor block for hydrocarbon synthesis includes a reactor 20 1500 mm high and 16 mm in diameter, equipped with a cooling jacket and a coaxial pocket for a thermocouple, and a steam collector 21. The volume of catalyst loaded into the reactor is 100 cm^3 (fraction 1–2 mm mixed with 100 cm^3 1–2 mm quartz).

The temperature in the catalytic zone is controlled by removing excess reaction heat due to the phase transition of water to steam in the cooling jacket or, in case of a lack of heat, by heating the water in the jacket using a heating furnace and a Termodat 38 temperature

controller. The parameters (T, P) of boiling water in the jacket are set by the pressure regulator 26. The pressure in the plant and the reactor is controlled by pressure gauge 9 and electronic pressure sensors 11 and 33. The reaction product cooling unit is a set of air-cooled separators 27 and 30 and a water cooler 29.

Before starting the catalytic tests, the catalyst was reduced in a hydrogen flow for 3 h at a temperature of 400 °C and a GHSV of 3000 h⁻¹. Activation of the samples with synthesis gas with a ratio of H₂/CO = 2 and catalytic tests were carried out at a pressure of 1.0 MPa and GHSV of 1000 h⁻¹, raising the temperature from 180 °C to the specified test temperature at a rate of 2.5 °C h⁻¹.

The production of an experimental batch of hydrocarbons of the gasoline fraction was carried out in a continuous mode of operation for 400 h. As collectors 27 and 30 were filled, the synthesis products (liquid C₅₊ hydrocarbons and water) were drained and subjected to separation, fractionation, and analysis. Since in the course of long-term testing, there is a partial loss of the hydrotreating function of the catalyst, accompanied by a decrease in the content of isomeric structures (iso-alkanes, iso-alkenes) that affect the quality and performance characteristics of the fuel, all hydrocarbon samples taken over 400 h of operation were combined and used to determine the average characteristics of the fuel.

In parallel with the production of synthetic hydrocarbons, the temperature was controlled along the height of the catalytic layer and, if necessary, corrected. The average temperature in the catalytic bed was maintained in the range of 247–250 °C, which ensured a CO conversion of at least 70%.

The composition of the initial gas and gaseous synthesis products was analyzed using a Kristall 5000 gas chromatograph (Khromatek, Russia) equipped with a thermal conductivity detector and two columns (Haysep R active phase and NaX molecular sieves). The analysis mode is temperature-programmable with a heating rate of 8 °C/min.

The condensed synthesis products were separated via distillation at atmospheric pressure, separating fuel fractions with a boiling point: gasoline—up to 180 °C, diesel—180–330 °C, distillation residue—above 330 °C. The composition of C₅₊ hydrocarbons was determined using an Agilent 7890A chromato-mass spectrometer (Agilent Technologies, Santa Clara, CA, USA) equipped with an MSD 5975C detector and an HP-5MS capillary column.

4. Conclusions

The conducted studies on the variation of technological parameters in the synthesis of FT on a bifunctional catalyst made it possible to identify the conditions under which the largest amount of gasoline fraction with the content of isomeric hydrocarbons is formed (pressure 1.0 MPa, temperature 250 °C, GHSV = 1000 h⁻¹). Under these conditions, an experimental batch of gasoline fraction was produced at the pilot plant; its main properties were analyzed according to GOST. The resulting synthetic fraction of gasoline fuel in some parameters differs significantly from the requirements of GOST 51105-2020 for petroleum gasoline. There are no aromatic hydrocarbons and benzene in the synthetic fraction, which improves its environmental characteristics but reduces its operational characteristics—octane number and density. According to the content of olefins, the synthetic gasoline fraction is close to catalytically cracked gasoline.

Thus, gasoline fuel obtained through the fractionation of synthetic oil certainly has good environmental characteristics, but in terms of performance, it does not meet the requirements of the current standards for petroleum gasoline. The use of synthetic gasoline may become possible by compounding it, for example, with distillates from secondary oil refining processes at refineries. At the same time, C₁–C₄ hydrocarbon gases, which are available in excess at refineries, can become raw materials for producing synthetic gasoline.

Another possible option for bringing synthetic gasoline to the requirements of GOST is its secondary processing, for example, light hydrogenation, catalytic reforming, and methoxylation processes. However, this requires additional research on the selection of catalysts and process modes.

Author Contributions: Project administration, R.E.Y.; Writing - original draft, G.B.N.; Investigation, I.N.Z.; Formal analysis, E.A.B.; Writing—review & editing, Y.V.K.; Methodology, R.D.S.; Conceptualization, A.P.S. All authors have read and agreed to the published version of the manuscript.

Funding: The study was carried out as part of the implementation of the national project “Science and Universities” under the support of the Ministry of Science and Higher Education Research Institute of the Russian Federation, project No. 075-03-2021-016/4 in the laboratory “New compositional and functional materials alas with special properties”.

Data Availability Statement: Not applicable.

Conflicts of Interest: The authors declare no conflict of interest.

References

1. Li, N.; Jiao, F.; Pan, X.; Chen, Y.; Feng, J.; Li, G.; Bao, X. High-quality gasoline directly from syngas by dual metal oxide–zeolite (OX-ZEO) catalysis. *Angew. Chem. Int. Ed.* **2019**, *58*, 7400–7404. [[CrossRef](#)] [[PubMed](#)]
2. Pan, X.; Jiao, F.; Miao, D.; Bao, X. Oxide–zeolite-based composite catalyst concept that enables syngas chemistry beyond Fischer–Tropsch synthesis. *Chem. Rev.* **2021**, *121*, 6588–6609. [[CrossRef](#)] [[PubMed](#)]
3. Lischiner, I.; Malova, O.; Tarasov, A.; Krotov, M.; Korobtsev, S.; Potapkin, B. Obtaining of Environmental Motor Fuel with Low Durene Content of Dimethyl Ether. *Ecol. Ind. Russ.* **2017**, *21*, 20–23. [[CrossRef](#)]
4. Khadzhiev, S.N.; Vytnova, L.A. The first commercial Fischer-Tropsch processes in Germany. *Pet. Chem.* **2008**, *48*, 133–149. [[CrossRef](#)]
5. Li, J.; He, Y.; Tan, L.; Zhang, P.; Peng, X.; Oruganti, A.; Yang, G.; Abe, H.; Wang, Y.; Tsubaki, N. Integrated tuneable synthesis of liquid fuels via Fischer–Tropsch technology. *Nat. Catal.* **2018**, *1*, 787–793. [[CrossRef](#)]
6. Keil, F.J. Methanol-to-hydrocarbons: Process technology. *Microporous Mesoporous Mater.* **1999**, *29*, 49–66. [[CrossRef](#)]
7. Topp-Jørgensen, J. Topsøe integrated gasoline synthesis—The TIGAS process. In *Studies in Surface Science and Catalysis*; Elsevier: Amsterdam, The Netherlands, 1988; Volume 36, pp. 293–305. [[CrossRef](#)]
8. Mysov, V.M.; Reshetnikov, S.I.; Stepanov, V.G.; Ione, K.G. Synthesis gas conversion into hydrocarbons (gasoline range) over bifunctional zeolite-containing catalyst: Experimental study and mathematical modelling. *Chem. Eng. J.* **2005**, *107*, 63–71. [[CrossRef](#)]
9. Fu, T.; Chang, J.; Shao, J.; Li, Z. Fabrication of a nano-sized ZSM-5 zeolite with intercrystalline mesopores for conversion of methanol to gasoline. *J. Energy Chem.* **2017**, *26*, 139–146. [[CrossRef](#)]
10. Matieva, Z.M.; Kolesnichenko, N.V.; Snatenkova, Y.M.; Maksimov, A.L. Conversion of syngas to triptane-rich liquid hydrocarbons via oxygenates. *Fuel* **2021**, *304*, 121407. [[CrossRef](#)]
11. Xing, C.; Li, M.; Zhang, G.; Noreen, A.; Fu, Y.; Yao, M.; Lu, C.; Gao, X.; Yang, R.; Amoo, C.C. Syngas to isoparaffins: Rationalizing selectivity over zeolites assisted by a predictive isomerization model. *Fuel* **2021**, *285*, 119233. [[CrossRef](#)]
12. Zhu, C.; Bollas, G.M. Gasoline selective Fischer-Tropsch synthesis in structured bifunctional catalysts. *Appl. Catal. B Environ.* **2018**, *235*, 92–102. [[CrossRef](#)]
13. Wang, C.; Fang, W.; Wang, L.; Xiao, F.S. Fischer-Tropsch reaction within zeolite crystals for selective formation of gasoline-ranged hydrocarbons. *J. Energy Chem.* **2021**, *54*, 429–433. [[CrossRef](#)]
14. Cheng, S.; Mazonde, B.; Zhang, G.; Javed, M.; Dai, P.; Cao, Y.; Tu, S.; Wu, J.; Lu, C.; Xing, C.; et al. Co-based MOR/ZSM-5 composite zeolites over a solvent-free synthesis strategy for improving gasoline selectivity. *Fuel* **2018**, *223*, 354–359. [[CrossRef](#)]
15. Javed, M.; Cheng, S.; Zhang, G.; Dai, P.; Cao, Y.; Lu, C.; Yang, R.; Xing, C.; Shan, S. Complete encapsulation of zeolite supported Co based core with silicalite-1 shell to achieve high gasoline selectivity in Fischer-Tropsch synthesis. *Fuel* **2018**, *215*, 226–231. [[CrossRef](#)]
16. Zhu, C.; Gamliel, D.P.; Valla, J.A.; Bollas, G.M. Fischer-Tropsch synthesis in monolith catalysts coated with hierarchical ZSM-5. *Appl. Catal. B Environ.* **2021**, *284*, 119719. [[CrossRef](#)]
17. Sineva, L.V.; Gorokhova, E.O.; Gryaznov, K.O.; Ermolaev, I.S.; Mordkovich, V.Z. Zeolites as a tool for intensification of mass transfer on the surface of a cobalt Fischer–Tropsch synthesis catalyst. *Catal. Today* **2021**, *378*, 140–148. [[CrossRef](#)]
18. Sineva, L.; Mordkovich, V.; Asalieva, E.; Smirnova, V. Zeolite-Containing Co Catalysts for Fischer–Tropsch Synthesis with Tailor-Made Molecular-Weight Distribution of Hydrocarbons. *Reactions* **2023**, *4*, 359–380. [[CrossRef](#)]
19. Kibby, C.; Jothimurugesan, K.; Das, T.; Lacheen, H.S.; Rea, T.; Saxton, R.J. Chevron’s gas conversion catalysis-hybrid catalysts for wax-free Fischer–Tropsch synthesis. *Catal. Today* **2013**, *215*, 131–141. [[CrossRef](#)]
20. Yakovenko, R.E.; Savost’yanov, A.P.; Narochnyi, G.B.; Soromotin, V.N.; Zubkov, I.N.; Papeta, O.P.; Svetogorov, R.D.; Mitchenko, S.A. Preliminary evaluation of a commercially viable Co-based hybrid catalyst system in Fischer-Tropsch synthesis combined with hydroprocessing. *Catal. Sci. Technol.* **2020**, *10*, 7613–7629. [[CrossRef](#)]
21. Yakovenko, R.E.; Zubkov, I.N.; Bakun, V.G.; Agliullin, M.R.; Saliev, A.N.; Savost’yanov, A.P. Bifunctional Cobalt Catalyst for the Synthesis of Waxy Diesel Fuel by the Fischer–Tropsch Method: From Development to Commercialization. Part 1: Selection of the Industrial Sample of the Zeolite Component HZSM-5. *Catal. Ind.* **2021**, *13*, 230–238. [[CrossRef](#)]

22. Narochnyi, G.B.; Yakovenko, R.E.; Savost'yanov, A.P.; Bakun, V.G. Experience in introducing a cobalt catalyst technology for the synthesis of hydrocarbons from CO and H₂. *Catal. Ind.* **2016**, *8*, 139–144. [[CrossRef](#)]
23. Savost'yanov, A.P.; Narochnyi, G.B.; Yakovenko, R.E.; Saliev, A.N.; Sulima, S.I.; Zubkov, I.N.; Nekroenko, S.V.; Mitchenko, S.A. Synthesis of low-pour-point diesel fuel in the presence of a composite cobalt-containing catalyst. *Petrol. Chem.* **2017**, *57*, 1186–1189. [[CrossRef](#)]
24. Adeleke, A.A.; Liu, X.; Lu, X.; Moyo, M.; Hildebrandt, D. Cobalt hybrid catalysts in Fischer-Tropsch synthesis. *Rev. Chem. Eng.* **2020**, *36*, 437–457. [[CrossRef](#)]
25. Gholami, Z.; Tišler, Z.; Rubáš, V. Recent advances in Fischer-Tropsch synthesis using cobalt-based catalysts: A review on supports, promoters, and reactors. *Catal. Rev.* **2021**, *63*, 512–595. [[CrossRef](#)]
26. Sineva, L.V.; Asalieva, E.Y.; Mordkovich, V.Z. The role of zeolite in the Fischer-Tropsch synthesis over cobalt-zeolite catalysts. *Russ. Chem. Rev.* **2015**, *84*, 1176. [[CrossRef](#)]
27. Sineva, L.V.; Nalivaiko, E.O.; Gryaznov, K.O.; Mordkovich, V.Z. Role of Zeolites in Heat and Mass Transfer in Pelletized Multifunctional Cobalt-Based Fischer-Tropsch Catalysts. *Kinet. Catal.* **2022**, *63*, 321–329. [[CrossRef](#)]
28. Yakovenko, R.E.; Zubkov, I.N.; Bakun, V.G.; Savost'yanov, A.P. Combined Synthesis and Hydroprocessing of Hydrocarbons over Co/SiO₂+ZSM-5+Al₂O₃ Catalysts Promoted by Nickel. *Pet. Chem.* **2021**, *61*, 516–526. [[CrossRef](#)]
29. Abdellatif, T.M.; Ershov, M.A.; Kapustin, V.M.; Abdelkareem, M.A.; Kamil, M.; Olabi, A.G. Recent trends for introducing promising fuel components to enhance the anti-knock quality of gasoline: A systematic review. *Fuel* **2021**, *291*, 120112. [[CrossRef](#)]
30. Blinova, I.O.; Glukhova, V.A. Features of ignition and combustion of fuels in gasoline engines. *Theory Pract. Mod. Sci.* **2020**, 9–11.
31. Ershov, M.; Potanin, D.; Guseva, A.; Abdellatif, T.M.; Kapustin, V.M. Novel strategy to develop the technology of high-octane alternative fuel based on low-octane gasoline Fischer-Tropsch process. *Fuel* **2020**, *261*, 116330. [[CrossRef](#)]
32. Yakovenko, R.E.; Zubkov, I.N.; Bakun, V.G.; Papeta, O.P.; Savostyanov, A.P. Effects of SiO₂/Al₂O₃ Ratio in ZSM-5 Zeolite on the Activity and Selectivity of a Bifunctional Cobalt Catalyst for Synthesis of Low-Pour-Point Diesel Fuels from CO and H₂. *Pet. Chem.* **2022**, *62*, 101–111. [[CrossRef](#)]
33. PDF-2. The Powder Diffraction File TM. International Center for Diffraction Data (ICDD). PDF-2 Release 2012. 2014. Available online: www.icdd.com (accessed on 10 August 2023).
34. Young, R.A. *The Rietveld Method*; Oxford University Press: Oxford, UK, 1995; 298p.
35. Schanke, D.; Vada, S.; Blekkan, E.A.; Hilmen, A.M.; Hoff, A.; Holmen, A. Study of Pt-promoted cobalt CO hydrogenation catalysts. *J. Catal.* **1995**, *156*, 85–95. [[CrossRef](#)]
36. Prieto, G.; Martínez, A.; Concepción, P.; Moreno-Tost, R. Cobalt particle size effects in Fischer-Tropsch synthesis: Structural and in situ spectroscopic characterisation on reverse micelle-synthesised Co/ITQ-2 model catalysts. *J. Catal.* **2009**, *266*, 129–144. [[CrossRef](#)]
37. Qie, Y.; Liu, Y.; Kong, F.; Yang, Z.; Yang, H. High coercivity cobalt carbide nanoparticles as electrocatalysts for hydrogen evolution reaction. *Nano Res.* **2022**, *15*, 3901–3906. [[CrossRef](#)]
38. Alex, P.; Majumdar, S.; Kishor, J.; Sharma, I.G. Synthesis of cobalt nanocrystals in aqueous media and its characterization. *Mater. Sci. Appl.* **2011**, *2*, 1307–1312. [[CrossRef](#)]

Disclaimer/Publisher's Note: The statements, opinions and data contained in all publications are solely those of the individual author(s) and contributor(s) and not of MDPI and/or the editor(s). MDPI and/or the editor(s) disclaim responsibility for any injury to people or property resulting from any ideas, methods, instructions or products referred to in the content.